Rare Metal Materials and Engineering
Volume 47, Issue 7, July 2018
Online English edition of the Chinese language journal

Available online at www.sciencedirect.com

ScienceDirect

Cite this article as: Rare Metal Materials and Engineering, 2018, 47(7): 1980-1985.

ARTICLE

Pre-deformation and Aging Characteristics of Cu-3Ti-2Mg Alloy

Liu Jia, Wang Xianhui, Ran Qianni, Liu Yanfeng, Li Cong

Shaanxi Key Laboratory of Electrical Materials and Infiltration Technology, Xi'an University of Technology, Xi'an 710048, China

Abstract: The effect of cold deformation and aging on the microstructure and properties of Cu-3Ti-2Mg alloy was investigated. The microstructure and phase constituents were characterized by optical microscope (OM), scanning electron microscope (SEM), X-ray diffractometer (XRD), transmission electron microscope (TEM) and electron backscattering diffraction (EBSD), and the hardness and electrical conductivity were measured as well. The results show that the microstructure of as-cast Cu-3Ti-2Mg alloy consists of Cu_2Mg phase, plate-like Cu_4Ti phase and Cu matrix. The microstructural characterizations reveal that the β'-Cu_4Ti phase precipitates from the supersaturated Cu matrix during aging. However, excessive aging causes the phase transformation from metastable, coherent β'-Cu_4Ti to equilibrium, incoherent Cu_3Ti phases. In the range of experiments, the optimum process for Cu-3Ti-2Mg alloy is solutizing at 700 °C for 4 h, cold deformation of 60%, and aging at 450 °C for 2 h. The electrical conductivity and hardness HV of Cu-3Ti-2Mg alloy are 16.7 %IACS and 3280 MPa, respectively.

Key words: Cu-Ti alloy; deformation; phase transformation; hardness; electrical conductivity

Copper alloys have been used as the electrical contacts, electrical connection and high-strength springs due to their high strength and good electrical conductivity[1,3]. Among these copper alloys, Cu-Be alloys are most widely used owing to their good mechanical and electrical properties[4]. However, the toxicity of beryllium in Cu-Be alloy is harmful to humanity health during manufacturing process. Furthermore, Cu-Be alloys have poor anti-stress relaxation property at elevated temperatures [5], so it is of great significance to develop a substituent for Cu-Be alloys. In past decades, a number of beryllium free copper alloys such as Cu-Ni-Sn[6,7], Cu-Ni-Si[8-10] and Cu-Ti alloys have been studied[11-15]. Because of good mechanical properties and excellent anti-stress relaxation property at elevated temperatures, Cu-Ti alloys are regarded as potential substitutes for Cu-Be alloys. Nevertheless, the Cu-Ti alloys present poor electrical conductivity since a large number of Ti solute atoms dissolve in the Cu matrix. Subsequently, it is necessary to decrease the solution of Ti atoms in the Cu-Ti alloys without deteriorating mechanical strength. So far, various kinds of the addition of alloying elements into Cu-Ti alloy have been reported [16-22]. Konno et al.[23] revealed that the electrical conductivity of Cu-3at%Ti alloy with the addition of 4at%Al is increased by six times higher than that without Al addition since the formation of $AlCu_2Ti$ phase decreases the solute Ti concentration in the Cu matrix. Our previous investigations also show that the addition of Ni into Cu-Ti alloys can improve the hardness and electrical conductivity since the formation of intermetallic compound decreases the solution of Ti atoms in the Cu matrix[24,25]. Maki et al.[26] reported that copper alloys exhibit high strength and electrical conductivity by Mg supersaturation solid-solution strengthening. Ito et al.[27] found that cold rolling can significantly improve the strength and electrical conductivity of supersaturated Cu-Mg alloy. Yang et al.[28] and Monzen et al.[29] believed that the increased strength of Cu based alloys is derived from the drag effect of Mg atoms on dislocation motion. In the present work, the effect of Mg

Received date: July 14, 2017
Foundation item: National Natural Science Foundation of China (51274163); Science and Technique Innovation Program of Shaanxi Province for Key Laboratory (2014SZS08-K02); Research Program of Shaanxi Provincial Key Laboratory (13JS076); Shaanxi Provincial Project of Special Foundation of Key Disciplines (2011HBSZS009)
Corresponding author: Wang Xianhui, Ph. D., Professor, School of Materials Science and Engineering, Xi'an University of Technology, Xi'an 710048, P. R. China, Tel: 0086-29-82312185, E-mail: xhwang693@xaut.edu.cn

addition on the microstructure and properties of Cu-3Ti alloy was studied by structural characterization and property tests. The purpose of the investigation is to clarify the relationship of hardness and electrical conductivity with microstructural evolution of Cu-3Ti-2Mg, and to develop a new environment-friendly alloy with a better combination of mechanical properties and electrical conductivity.

1 Experiment

The starting materials were 99.9 wt% electrolytic copper, 99.9 wt% sponge titanium, and 99.99 wt% Cu-15Mg master alloys. An ingot of Cu-3wt%Ti-2wt%Mg alloy was prepared in a non-consumable vacuum arc furnace. For convenience, the Cu-3wt%Ti-2 wt%Mg alloy was designated as Cu-3Ti-2Mg alloy. The ingot was sliced into the specimens with a diameter of 15 mm and length of 10 mm. These specimens were solutized at 700 °C for 4 h in argon atmosphere, followed by quenching in water. Then, the specimens were cold-rolled with deformation by 20%, 40%, 60% and 80%, followed by aging at 450 °C for 1, 2, 3 and 4 h under the protection of argon atmosphere. The specimens for microstructural examination were mechanically polished and subsequently electrochemically etched in a 30 wt% phosphoric alcohol solution. The microstructures were characterized by a GX71 optical microscope (OM) and a JSM-6700F field-emission scanning electron microscope (SEM). The phase constituents and structure of the alloy were characterized using a XRD-7000S X-ray diffractometer (XRD) and a Zeiss-Merlin SEM equipped with an Oxford Instruments *hkl* channel 5 electron backscattering diffraction (EBSD) system. Data was acquired under the scanning step size of 1 μm. The samples for EBSD analysis were prepared by mechanical polishing with subsequent vibratory polishing for 3 h. The morphology of the precipitates was characterized by a JEM-2100HR transmission electron microscope (TEM). The specimens used for TEM observations were cut from the aged samples and then mechanically polished to obtain 40~60 μm thick slices. Discs of 3 mm in diameter were punched from these slices and then thinned in a M691 ion milling machine at 4.5 kV. Hardness were determined on a TUKON2100 microhardness tester, with a load of 50 g and holding time of 10 s. Electrical conductivity were measured at FQR-7501 eddy conductivity gauge, and the values are the average of five times measured results.

2 Results and Discussion

2.1 OM, SEM and XRD characterization

Fig.1 is the XRD pattern of as-cast Cu-3Ti-2Mg alloy. It is learnt that the Cu-3Ti-2Mg alloy consists of Cu_2Mg phase and Cu matrix. Fig.2 is the microstructure of as-cast Cu-3Ti-2Mg alloy. Evidently, plate-like phases are located among the dendrites. It is verified by energy dispersive spectrum (EDS) analysis that they are Cu_4Ti phase, as shown in Fig.3 and Table 1.

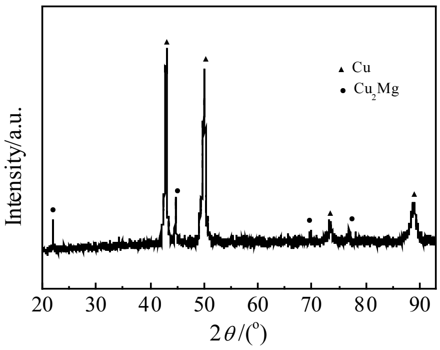

Fig.1 XRD pattern of as-cast Cu-3Ti-2Mg alloy

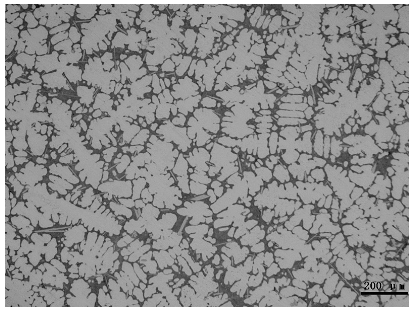

Fig.2 OM micrograph of as-cast Cu-3Ti-2Mg alloy

Fig.4 shows the cross-sectional microstructures of Cu-3Ti-2Mg alloy after different cold deformation and aging at 450 °C for 4 h. As seen from Fig.4a, no obvious lamellar precipitate appears after 20% cold-rolling deformation and aging. After 40% cold deformation and aging, a shorter, discontinuous lamellar precipitates emerge inside the grains (Fig.4b). However, the lamellar precipitates become longer and continuous after 60% cold-rolling deformation and aging (Fig. 4c). After 80% cold-rolling deformation and aging, the lamellar precipitates inside grains become more continuous (Fig.4d).

Fig.5 shows the longitudinal microstructures of Cu-3Ti-2Mg alloy after different cold deformation and aging at 450 °C for 4 h. As seen from Fig.5, the equiaxial grains are elongated with increase of cold-rolling deformation.

2.2 TEM characterization

To further clarify the size and morphology of the precipitates of the aged Cu-3Ti-2Mg alloy, two specimens after 60% cold-rolling deformation and aging at 450 °C for 1 and 4 h were characterized by TEM (see Fig.6 and Fig.7). Fig.6a is the bright-field (BF) TEM image of Cu-3Ti-2Mg

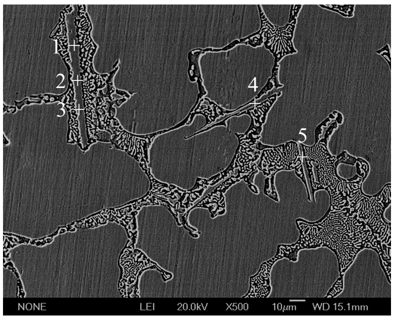

Fig.3 SEM micrograph of as-cast Cu-3Ti-2Mg alloy

Table 1 EDS result of stripe phase marked positions 1~5 in Fig.3 (at%)

Position	Cu	Ti	Mg
1	80.21	19.66	0.13
2	80.31	19.63	0.06
3	79.84	19.98	0.18
4	80.18	19.56	0.26
5	79.45	20.31	0.24

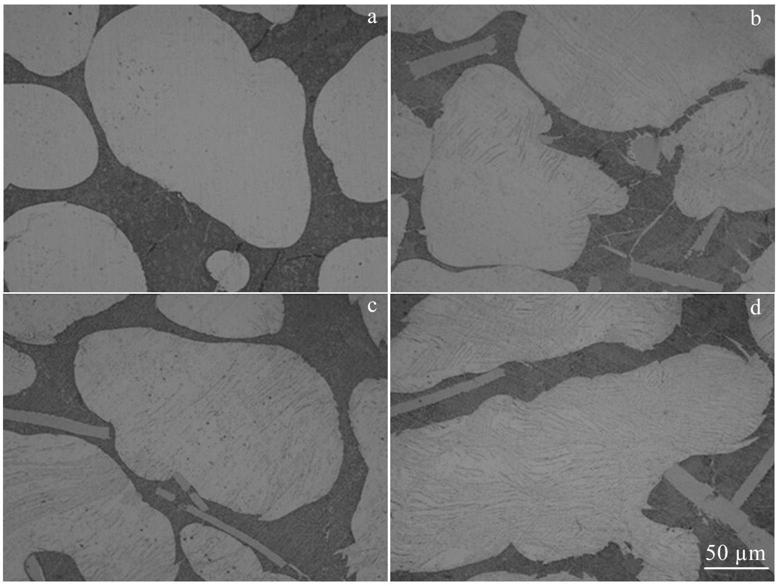

Fig.4 Cross-sectional microstructures of Cu-3Ti-2Mg alloy after different cold deformations and aging at 450 °C for 4 h: (a) 20%, (b) 40%, (c) 60%, and (d) 80%

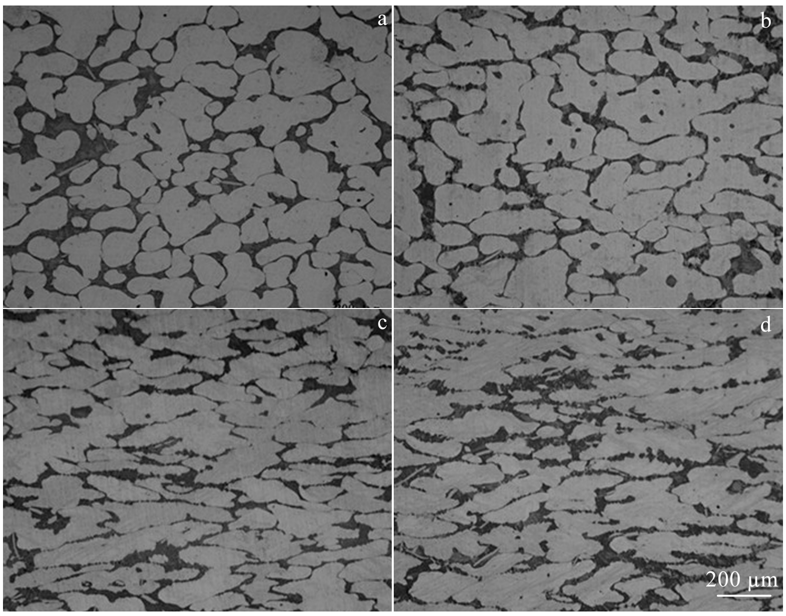

Fig.5 Longitudinal microstructures of Cu-3Ti-2Mg alloy after different cold deformations and aging at 450 °C for 4 h: (a) 20%, (b) 40%, (c) 60%, and (d) 80%

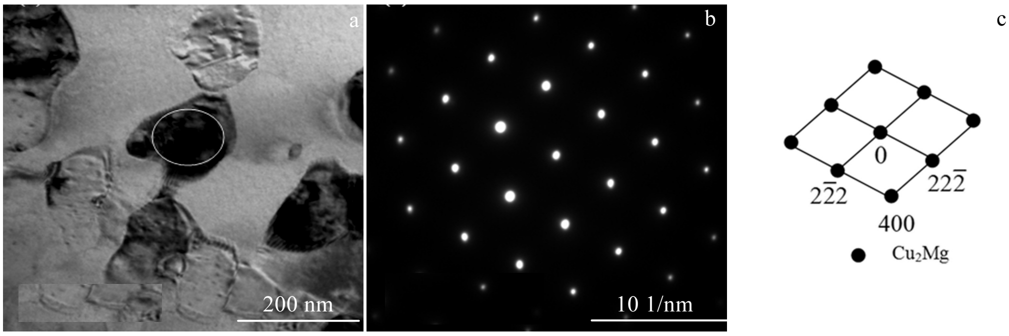

Fig.6 TEM image (a), SAED pattern (b) and schematic (c) of Cu-3Ti-2Mg alloy after 60% cold deformation and aging at 450 °C for 1 h

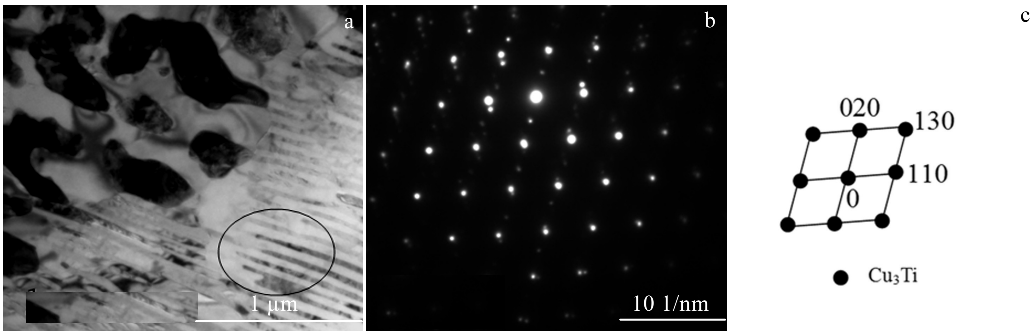

Fig.7 TEM image (a), SAED pattern (b) and schematic (c) of Cu-3Ti-2Mg alloy after 60% cold deformation and aging at 450 °C for 4 h

alloy at low magnification. As seen from Fig. 6a, the precipitate has a size of approximately 100~200 nm. Its selected area electron diffraction (SAED) pattern and schematic diagram are shown in Fig.6b and 6c. It can be determined from Fig.6b and 6c that the precipitate is Cu_2Mg phase having a cubic structure with the lattice parameters: $a = b = c = 0.7047$ nm.

Fig.7a~7c are the BF image of Cu-3Ti-2Mg alloy after 60% cold deformation and aging at 450 °C for 4 h at low magnification, the corresponding SAED pattern and its schematic diagram, respectively. It is noticed that there are lamellar phases besides the Cu_2Mg phase. As determined from Fig.7b and 7c, the lamellar phase is Cu_3Ti, having an orthorhombic structure with lattice parameters: $a = 0.2585$ nm, $b = 0.4527$ nm, $c = 0.4351$ nm. Sembishi et al.[30,31] reported that Ti-rich α' continuously transforms into the metastable, coherent β'-Cu_4Ti phase during aging. With prolonged aging, β'-Cu_4Ti phases progressively transform into equilibrium, incoherent Cu_3Ti phases.

2.3 EBSD characterization

The distribution and volume fraction of the phase of the aged Cu-3Ti-2Mg alloy were evaluated by EBSD. Fig.8 shows the phase distribution of the Cu-3Ti-2Mg alloy after 60% cold deformation and aging at 450 °C for 4 h. Evidently, the aged Cu-3Ti-2Mg alloy consists of Cu_2Mg, Cu_4Ti, Cu_3Ti and Cu matrix. Cu_2Mg phase is distributed in the Cu matrix, while Cu_4Ti and Cu_3Ti phase are located at the grain boundary. The volume fraction of Cu_2Mg, Cu_4Ti and Cu_3Ti phase are 20.86%, 0.25% and 2.71%, respectively.

2.4 Electrical conductivity and hardness

Fig.9 shows the variation of the electrical conductivity and hardness of Cu-3Ti-2Mg alloy aged at 450 °C for 4 h with deformation. As seen from Fig.9, the electrical conductivity increases and then decreases with increase of deformation. The maximum electrical conductivity of 16.0%IACS can be obtained after 60% cold deformation and aging at 450 °C for 4 h. It is generally believed that more distortion energy promotes phase precipitation[32,33]. Hence, these Ti and Mg solute atoms decrease significantly in the Cu matrix and reduce the electron scattering, thus giving rise to the increase of the electrical conductivity. Nevertheless, the larger deformation increases lattice distortion and electron scattering significantly, resulting in the decrease of the electrical conductivity.

It can also be seen that the hardness increases gradually with increase of cold deformation, since larger distortion energy promotes the full precipitation of secondary phase. In addition, the sharply increased dislocation density triggers the interaction of the dislocation and the elastic

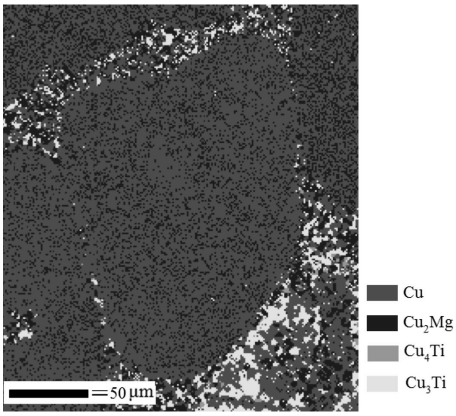

Fig.8 EBSD image of cross-sectional microstructure of Cu-3Ti-2Mg alloy after 60% cold deformation and aging at 450 °C for 4 h

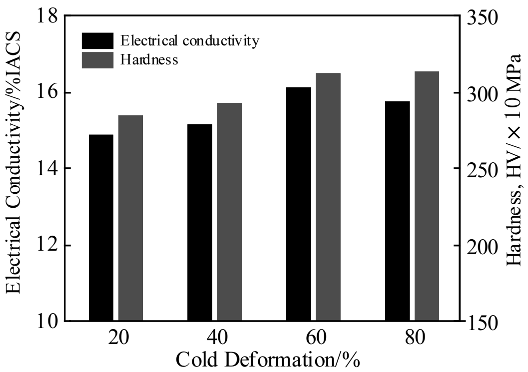

Fig.9 Variation of the electrical conductivity and hardness HV of Cu-3Ti-2Mg alloy after different cold deformation and aging at 450 °C for 4 h

stress, which further hinders the dislocation motion, thus causing the increase of hardness.

Fig. 10 is the effect of aging time on the electrical conductivity and hardness of Cu-3Ti-2Mg alloy after 60% cold deformation. As seen from Fig.10, the electrical conductivity and hardness increase and then decrease slightly with aging time. The peak electrical conductivity and hardness HV can be achieved after aging at 450 °C for 2 h, which are 16.7 %IACS and 3280 MPa, respectively. In comparison with solid solution Cu-3Ti-2Mg alloy, the electrical conductivity and hardness are increased by 203.6% and 143.0%, respectively.

The solubility of alloying elements in the Cu matrix is a dominant factor to affect the electrical conductivity of Cu-3Ti-2Mg alloy. With the progressive precipitates from the supersaturated Cu matrix during aging, the lattice distortion and electron scattering decrease significantly,

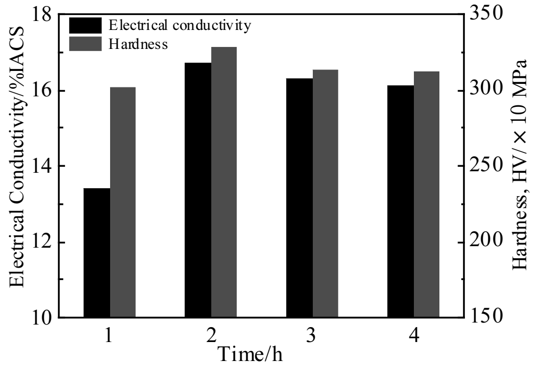

Fig.10 Influence of aging time on the electrical conductivity and hardness of Cu-3Ti-2Mg alloy with 60% cold deformation

thus leading to the increase of the electrical conductivity. However, excessive aging causes the coarsening of precipitates and partial re-dissolution of alloying elements into the Cu matrix, which decrease the electrical conductivity.

The coherent and metastable β'-Cu_4Ti phase is favorable for the improvement on the hardness of Cu-3Ti-2Mg alloy after an appropriate aging. However, excessive aging causes the phase transformation from the coherent and metastable β'-Cu_4Ti phase to incoherent and equilibrium Cu_3Ti phases, thus resulting in the decrease of hardness. It should be noted that the electrical conductivity and hardness of Cu-3Ti-2Mg alloy are close to those of the commercial QBe2.0 alloy, which has the electrical conductivity ≥18 %IACS and hardness ≥3600 MPa [34].

3 Conclusions

1) As-cast Cu-3Ti-2Mg alloy consists of Cu_2Mg phase, plate-like Cu_4Ti phase and Cu matrix.

2) Appropriate deformation is beneficial for the improvement on the electrical conductivity and hardness, but the larger deformation increases lattice distortion and electron scattering significantly, resulting in the decrease of the electrical conductivity.

3) Aging promotes the precipitate of β'-Cu_4Ti phase. However, excessive aging causes the phase transformation from metastable, coherent β'-Cu_4Ti to equilibrium, incoherent Cu_3Ti phase, giving rise to the decrease of hardness.

4) In the range of the experiments, the optimum process for Cu-3Ti-2Mg alloy is solution treating at 700 °C for 4 h, 60% cold deformation and aging at 450 °C for 2 h. The electrical conductivity and hardness HV of Cu-3Ti-2Mg alloy are 16.7 %IACS and 3280 MPa, respectively.

References

1 Shen Y, Xie M, Bi J *et al. Rare Metal Materials and Engineering*[J], 2016, 45(8): 1997
2 Qin J, Yang X Y, Ye Y X *et al. Rare Metal Materials and Engineering*[J], 2016, 45(5): 1340 (in Chinese)
3 Xiang C J, Li H Q, Chen Z P *et al. Rare Metal Materials and Engineering*[J], 2016, 45(4): 1024 (in Chinese)
4 Zhou Y J, Song K X, Xing J D *et al. Journal of Alloys and Compounds*[J], 2016, 658: 920
5 Lei Q, Li Z, Dai C *et al. Materials Science and Engineering A*[J], 2013, 572(10): 65
6 Li X N, Wang M, Zhao L R *et al. Applied Surface Science*[J], 2014, 297: 89
7 Jeon W S, Shur C C, Kim J G *et al. Journal of Alloys and Compounds*[J], 2008, 455(1-2): 358
8 Lei Q, Li Z, Wang M P *et al. Journal of Alloys and Compounds*[J], 2011, 509(8): 3617
9 Suzuki S, Shibutani N, Mimura K *et al. Journal of Alloys and Compounds*[J], 2006, 417(1-2): 116
10 Xiao X P, Yi Z Y, Chen T T *et al. Journal of Alloys and Compounds*[J], 2016, 660: 178
11 Soffa W A, Laughlin D E. *Progress in Materials Science*[J], 2004, 49(3-4): 347
12 Nagarjuna S, Srinivas M, Balasubramanian K *et al. Materials Science and Engineering A*[J], 1999, 259(1): 34
13 Semboshi S, Al-Kassab T, Gemma R *et al. Ultramicroscopy*[J], 2009, 109(5): 593
14 Suzuki S, Hirabayashi K, Shibata H *et al. Scripta Materialia*[J], 2003, 48(4): 431
15 Markandeya R, Nagarjuna S, Sarma D S. *Materials Science and Engineering A*[J], 2005, 404(1-2): 305
16 Markandeya R, Nagarjuna S, Sarma D S. *Materials Science and Engineering A*[J], 2004, 371(1-2): 291
17 Markandeya R, Nagarjuna S, Sarma D S. *Materials Characterization*[J], 2006, 57(4-5): 348
18 Kim S, Kang M. *Journal of Industrial and Engineering Chemistry*[J], 2012, 18(3): 969
19 Markandeya R, Nagarjuna S, Sarma D S. *Journal of Materials Science*[J], 2004, 39(5): 1579
20 Wang X H, Chen C Y, Guo T T *et al. Journal of Materials Engineering and Performance*[J], 2015, 24(7): 2738
21 Lebreton V, Pachoutinski D, Bienvenu Y. *Materials Science and Engineering A*[J], 2009, 508(1-2): 83
22 Božića D, Dimčićb O, Dimčića B *et al. Materials characterization*[J], 2008, 59(8): 1122
23 Konno T J, Nishio R, Semboshi S *et al. Journal of Materials Science*[J], 2008, 43(11): 3761
24 Liu , Wang X , Guo T T *et al. International Journal of Minerals Metallurgy and Materials*[J], 2015, 22(11): 1199
25 Liu, Wang X, Guo T T *et al. Rare Metal Materials and Engineering*[J], 2016, 45(5): 1162
26 Maki K, Ito Y, Matsunaga H *et al. Scripta Materialia*[J], 2013, 68(10): 777
27 Ito Y, Matsunaga H, Mori H. *Materials Transactions*[J], 2014, 55(11): 1738
28 Yang G, Li Z, Yuan Y *et al. Journal of Alloys and Compounds*[J], 2015, 640: 347
29 Monzen R, Watanabe C. *Materials Science and Engineering A*[J], 2008, 483: 117
30 Semboshi S, Sato S, Ishikuro M *et al. Metallurgical and Materials Transactions A*[J], 2014, 45A: 3401
31 Markandeya R, Nagarjuna S, Satyanarayana D V V *et al. Materials Science and Engineering A*[J], 2006, 428(1-2): 233
32 Shen Y, Yang Y C, Zhang G Q *et al. Rare Metal Materials and Engineering*[J], 2014, 43(7): 1748 (in Chinese)
33 Markandeya R, Nagarjuna S, Sarma D S. *Materials Characterization*[J], 2005, 54: 360
34 Liu P, Ren F Z, Jia S G. *Copper Alloys and Applications*[M]. Beijing: Chemical Industry Press, 2007: 110 (in Chinese)

Cu-3Ti-2Mg 合金的时效特征

刘 佳，王献辉，冉倩妮，刘彦峰，李 聪
(西安理工大学 陕西省电气材料和渗透技术重点实验室，陕西 西安 710048)

摘 要：研究了冷变形及时效处理对Cu-3Ti-2Mg合金组织与性能的影响。采用光学显微镜(OM)、扫描电子显微镜(SEM)、X射线衍射仪(XRD)、透射电子显微镜(TEM)及电子背散射衍射(EBSD)对Cu-3Ti-2Mg合金的组织和析出相进行了表征，并对其硬度和导电率进行了测试。结果表明：铸态Cu-3Ti-2Mg合金由Cu_2Mg相、板条状Cu_4Ti相及Cu基体组成。时效处理后析出β'-Cu_4Ti相，过时效则会导致亚稳定β'-Cu_4Ti相转变为稳定的Cu_3Ti相。在本实验范围内，Cu-3Ti-2Mg合金的最佳热处理工艺是 700 ℃ 保温4 h后水淬，随后冷变形60%并在450 °C保温2 h炉冷。Cu-3Ti-2Mg合金的导电率及硬度HV分别是16.7 %IACS和3280 MPa。

关键词：铜合金；变形；相变；硬度；电导率

作者简介：刘 佳，女，1987 年生，博士生，西安理工大学材料科学与工程学院， 陕西 西安 710048，电话：029-82312185，E-mail: liujia09200920@163.com